Optimistic Reinforcement Learning by Forward Kullback-Leibler Divergence Optimization

Taisuke Kobayashi*

Nara Institute of Science and Technology, Nara, Japan

Abstract

This paper addresses a new interpretation of reinforcement learning (RL) as reverse Kullback-Leibler (KL) divergence optimization, and derives a new optimization method using forward KL divergence. Although RL originally aims to maximize return indirectly through optimization of policy, the recent work by Levine has proposed a different derivation process with explicit consideration of optimality as stochastic variable. This paper follows this concept and formulates the traditional learning laws for both value function and policy as the optimization problems with reverse KL divergence including optimality. Focusing on the asymmetry of KL divergence, the new optimization problems with reverse KL divergence including optimality. Focusing on the asymmetry of KL divergence, the new optimization problems with reverse KL divergence including optimality. Focusing on the asymmetry of KL divergence, the new optimization problems with reverse KL divergence including optimality. Focusing on the asymmetry of KL divergence, the new optimization problems with reverse KL divergence including optimality. Focusing on the asymmetry of KL divergence, the new optimization problems with reverse KL divergence includes an uncertainty parameter. In addition, it can be enhanced when it is integrated with proirtized experience replay and eligibility traces, both of which accelerate learning. The effects of this expected optimism was investigated through learning tendencies on numerical simulations using Pybullet. As a result, moderate optimism accelerate learning and yielded higher rewards. In a realistic robotic simulation with the moderate optimism outperformed one of the state-of-the-art RL method. Keywords:

Reinforcement learning (RL) (Sutton and Barto, 2018)

1. Introduction

Reinforcement learning (RL) (Sutton and Barto, 2018)

2. Introduction

Reinforcement learning (RL) (Sutton and Barto, 2018)

3. Interns of sample efficiency, reuse of experience replay (Lin, 1992; Schaul et al., 2015; Andrychowicz et al., 2017) and modelbased This paper addresses a new interpretation of reinforcement learning (RL) as reverse Kullback-Leibler (KL) divergence optimization, and derives a new optimization method using forward KL divergence. Although RL originally aims to

efficiency, have been central topics. For example, in terms of learning stability, frameworks for reducing the estimation bias of value function (Schulman et al., 2016; Fujimoto et al., 2018; Vuong and Tran, 2019; Kobayashi and Ilboudo, 2021) and regularization techniques for policy updates (Schulman et al., 2015; Munos et al., 2016; Haarnoja et al., 2018; Parisi et al., 2019; Schulman et al., 2017) have been widely proposed, and they have succeeded in reducing

*Corresponding author Email address: kobayashi@is.naist.jp (Taisuke Kobayashi) URL: http://kbys_t.gitlab.io/en/ (Taisuke Kobayashi)

perspectives.

In this direction, RL as probabilistic inference, as proposed by Levine (2018), stands on a very important position. It allows existing optimal control problems including RL to be interpreted as inference problems by explicitly giving the optimality as binary stochastic variable. For example, a soft actor critic (SAC) algorithm has been re-derived in the original paper, and new learning algorithms, such as policy optimization with stochastic latent space (Lee et al., 2020) and variational-inference-based model predictive control (Okada and Taniguchi, 2020), have also been proposed using this concept.

With this concept, this paper reveals that the optimizations of both value function and policy on the traditional RL are consistent with reverse Kullback-Leibler (KL) divergence optimization (named RKL-RL in this paper). That is, a new interpretation, RL as divergence optimization, is suggested. According to this suggestion, a new optimization method, so-called FKL-RL, is formulated based on forward KL divergence optimization. Note that, only regarding the policy optimization, it is pointed out that traditional RL uses reverse KL divergence, while imitation learning uses forward KL divergence (Ke et al., 2019; Uchibe and Doya, 2020).

These two types of optimization problems yield similar but different learning laws. One remarkable difference is optimism in FKL-RL. The optimism in the traditional RL has been implemented by several ways: such as the optimistic initialization of value function (Machado et al., 2015; Rashid et al., 2020); and the use of upper confidence (Sunehag and Hutter, 2015; Curi et al., 2020). Indeed, biological decision making has also been suggested to be optimistic RL (Lefebvre et al., 2017), which has asymmetric learning rates. Although these are given based on the traditional RL with several modifications, FKL-RL naturally possesses that property. This optimism can be controlled by a heuristic design of an uncertainty parameter left only in FKL-RL. In addition, FKL-RL integrated with prioritized experience replay (Schaul et al., 2015) and/or eligibility traces (Sutton and Barto, 2018), both of which are well-known to accelerate learning, would make the optimism enhance.

To investigate the effects of this expected optimism, numerical simulations using Pybullet (Coumans and Bai, 2016) are conducted with RKL-RL and FKL-RL. Their learning tendencies indicates that optimism gained by FKL-RL certainly enables the agent to escape from local optima, although too much optimism increases the variance of learning results, as in the case of policy gradient methods without a baseline term (Greensmith et al., 2004). In a more practical robot simulation, FKL-RL is able to obtain performance better than one of the latest methods (Schulman et al., 2017).

The contributions in this paper are three folds.

- 1. The traditional RL was proved as the optimization problem with reverse KL divergence.
- 2. FKL-RL was newly derived by considering another divergence (i.e. forward KL divergence) optimization
- The biological optimism was found in FKL-RL as the remarkable difference from RKL-RL, and experimentally investigated through numerical simulations.

RL as optimization problem with one of the divergences, as derived in this paper, may become a new step towards breakthrough in the traditional RL.

2. Preliminaries

2.1. Traditional reinforcement learning

The purpose of the traditional RL is to optimize policy so that the accumulation of rewards in the future (so-called return) is maximized (Sutton and Barto, 2018). This problem can be solved in Markov decision process (MDP) with the tuple (S, A, R, p_0, p_e) . Specifically, MDP assumes the following process. The state $s \in \mathcal{S}$ is first sampled from environment with either of probabilities, $s \sim p_0(s)$ as the initial random state or $s \sim p_e(s' \mid s, a)$ as the state transition. According to s, an agent decides the action $a \in \mathcal{A}$, using the learnable policy $a \sim \pi(a \mid s)$. a acts on the environment and stochastically updates the state to the next one $s' \sim p_e(s' \mid s, a)$. At that time, the agent obtains a reward $r \in \mathcal{R}$ from the environment: r = r(s, a). By repeating this process with the experienced data $(s, a, s^p rime, r)$, the agent obtains the following return R_t from the current time step t.

$$R_t = \sum_{k=0}^{\infty} \gamma^k r_{t+k} \tag{1}$$

where $\gamma \in [0,1)$ denotes the discount factor. Note that, by multiplying R_t with $(1-\gamma)$, the scale of return can be normalized to the scale of reward while holding the optimization problem.

Under this MDP, the optimization problem of $\pi(a \mid s)$ is given as follows:

$$\pi^*(a \mid s) = \arg\max_{\pi} \mathbb{E}_{p_e,\pi}[R_t \mid s_t = s]$$
 (2)

Here, the expected value of return is utilized since the future rewards are not deterministically given.

2.1.1. Value function optimization by Bellman equation

To solve the above optimization problem, state/action value functions are defined to estimate the expected return as $V(s) = \mathbb{E}_{p_e,\pi}[R_t \mid s_t = s]$ and $Q(s,a) = \mathbb{E}_{p_e,\pi}[R_t \mid s_t = s, a_t = a]$, respectively. Note that these two have the relationship, $V(s) = \mathbb{E}_{\pi}[Q(s,a)]$. If we know the current value, we can solve the above problem by simply taking actions that yield best (or better at least) values.

The value function can be learned according to Bellman equation, which focuses on the recursive relationship of return.

$$V(s) = \mathbb{E}_{p_e,\pi}[r_t] + \gamma \mathbb{E}_{p_e,\pi}[\sum_{k=0}^{\infty} \gamma^k r_{t+1+k} \mid s_{t+1} \sim p_e(s' \mid s = s_t, a = a_t)]$$

$$\simeq r_t + \gamma V(s' = s_{t+1})$$
(3)

where the last approximation is given by one-step Monte Carlo method. Since the value function holding this recursive equation is accurate, V(s) can be learned by minimizing temporal difference (TD) error, $\delta(s,a) := r + \gamma V(s') - \gamma V(s')$

V(s), as follows:

$$V^*(s) = \arg\min_{V(s)} \frac{1}{2} \delta^2(s, a)$$
 (4)

In RL with deep neural networks, $r + \gamma V(s')$ is regarded as the target signal and generated from target network like Kobayashi and Ilboudo (2021) did. Note that there are several variants such as Q-learning (Sutton and Barto, 2018), but they are not discussed in this paper for brevity.

2.1.2. Policy optimization by policy gradient

Using the value function, the policy can directly be optimized via eq. (2). That is, the following maximization problem is solved by the gradients w.r.t. the policy.

$$\pi^*(a \mid s) = \arg\max_{\pi} \mathbb{E}_{\pi}[Q(s, a) - V(s)]$$
$$\nabla \mathbb{E}_{\pi}[Q(s, a) - V(s)] = \mathbb{E}_{\pi}[(Q(s, a) - V(s))\nabla \ln \pi(a \mid s)]$$
(5)

Note that V(s) in the first line is added to reduce variance of learning (Greensmith et al., 2004), although its gradient is expected to be zero analytically. This optimization form is well-known as the actor-critic method (Sutton and Barto, 2018).

2.2. Forward/reverse Kullback-Leibler divergence

KL divergence is one of the famous divergence measures between two probability distributions (Kullback, 1997). Given p(x) and q(x) as the probabilities for stochastic variable x, KL divergence is defined as follows:

$$KL(p(x) \mid q(x)) := \int_{x} p(x) \ln \frac{p(x)}{q(x)} dx$$
 (6)

where the integral operation is given only when p and q are continuous (i.e. probability density functions), and switched to the summation operation when they are discrete (i.e. probability mass functions).

As can be seen in the above definition, KL divergence is asymmetry: $\mathrm{KL}(p(x) \mid q(x)) \neq \mathrm{KL}(q(x) \mid p(x))$. Therefore, in particular when considering optimization problems with KL divergence, we often distinguish forward or reverse KL divergence by which a target, p(x), and a model to be optimized, q(x), are entered into left or right side.

$$\begin{cases}
KL(p(x) \mid q(x)) & \text{Forward} \\
KL(q(x) \mid p(x)) & \text{Reverse}
\end{cases}$$
(7)

3. Proposal

3.1. Introduction of optimality

Levine (2018) has proposed a new interpretation of RL as probabilistic inference. With reference to the paper, an optimal variable $O = \{0,1\}$ is introduced. For simplicity, this paper supposes that O represents the optimality from

the current state to the future. That is, probability mass functions, $p(O=1\mid s)$ and $p(O=1\mid s,a)$, can be assumed as the functions of V(s) and Q(s,a), respectively. Specifically, in this paper, exponential function with an uncertainty parameter $\tau>0$ is employed as follows:

$$p(O=1 \mid s) = \exp\left(\frac{V(s) - C}{\tau}\right) =: p_V(s)$$
 (8)

$$p(O = 1 \mid s, a) = \exp\left(\frac{Q(s, a) - C}{\tau}\right) =: p_Q(s, a)$$
 (9)

where C is a constant to satisfy $V(s)-C\leq 0$ and $Q(s,a)-C\leq 0$ for $p(O)\in (0,1)$. Note that the boundary (i.e. 0 and 1) is excluded since it is infeasible to make the current situation perfectly optimal or non-optimal. With this natural assumption, all the following operations can be performed without exception. Since O is binary, the probability of O=0 can be given as $p(O=0\mid s)=1-p_V(s)$ and $p(O=0\mid s,a)=1-p_Q(s,a)$.

Using these probabilities, the optimal and non-optimal policies are defined. Specifically, Bayesian theorem for $\pi(a \mid s, O)$ derives the following relationship with the baseline policy $b(a \mid s)$, which is used for sampling actions.

$$\pi(a \mid s, O) = \frac{p(O \mid s, a)b(a \mid s)}{p(O \mid s)}$$

$$= \begin{cases} \frac{p_Q(s, a)}{p_V(s)}b(a \mid s) =: \pi^+(a \mid s) & O = 1\\ \frac{1 - p_Q(s, a)}{1 - p_V(s)}b(a \mid s) =: \pi^-(a \mid s) & O = 0 \end{cases}$$
(10)

3.2. Minimization of KL divergences between two optimal probabilities

Here, the optimization of the value function V(s) is considered. Note that if Q(s,a) is desired to be optimized directly, we may use the same derivation procedure combined with the fact $V(s) = \mathbb{E}_{\pi}[Q(s,a)]$.

It is essential to back-propagate the information increased by the addition of action a (and reward r returned as a result of a) as a condition to the probability where a is not included in the condition. This can be achieved by updating $p(O \mid s)$, which is the function of V, so as to minimize divergence between $p(O \mid s, a)$ and $p(O \mid s)$. As representative measure of divergence, this paper employs forward/reverse KL divergences, as mentioned in the introduction.

3.2.1. Reverse KL divergence

First, we consider the following minimization problem with reverse KL divergence.

$$\min \mathbb{E}_{p_e,b}[\mathrm{KL}(p(O \mid s) \mid p(O \mid s,a))] \tag{11}$$

When V(s) is parameterized by θ , the gradient of the reverse KL divergence, which is inside the expectation, over θ , g_{θ}^{R} , is derived as follows:

$$g_{\theta}^{R} = \nabla_{\theta} p_{V}(s) \ln \frac{p_{V}(s)}{p_{Q}(s,a)} - \nabla_{\theta} p_{V}(s) \ln \frac{1 - p_{V}(s)}{1 - p_{Q}(s,a)} + p_{V}(s) \nabla_{\theta} \ln p_{V}(s) + (1 - p_{V}(s)) \nabla_{\theta} \ln (1 - p_{V}(s))$$

$$= -g_{\theta}^{V} \frac{p_{V}(s)}{\tau} \left\{ \frac{Q(s,a) - V(s)}{\tau} + \ln \frac{1 - p_{V}(s)}{1 - p_{Q}(s,a)} \right\}$$

$$\propto -g_{\theta}^{V} \left\{ (Q(s,a) - V(s)) + \tau \ln \frac{1 - p_{V}(s)}{1 - p_{Q}(s,a)} \right\}$$
(12)

where $g_{\theta}^{V} = \nabla_{\theta} V(s)$ for simplicity. The two terms in the second line cancel each other out. The last proportion is given by multiplying the third line by $\tau^{2} p_{V}(s)^{-1}$.

Unfortunately, the above gradient cannot be computed due to the existence of C inside $p_V(s)$ and $p_Q(s,a)$. C is defined as the constant, but in general, its value is task-specific and unknown. Therefore, by considering the limit of $\tau \to 0$, g_{θ}^R can be approximated in a computable way.

$$g_{\theta}^{R} \simeq -g_{\theta}^{V}(Q(s, a) - V(s))$$
 (13)

As a remark, this gradient is equivalent with one for the squared error shown in eq. (4). In other words, the update law of the value function in the traditional RL can be regarded as the minimization problem of the reverse KL divergence.

3.2.2. Forward KL divergence

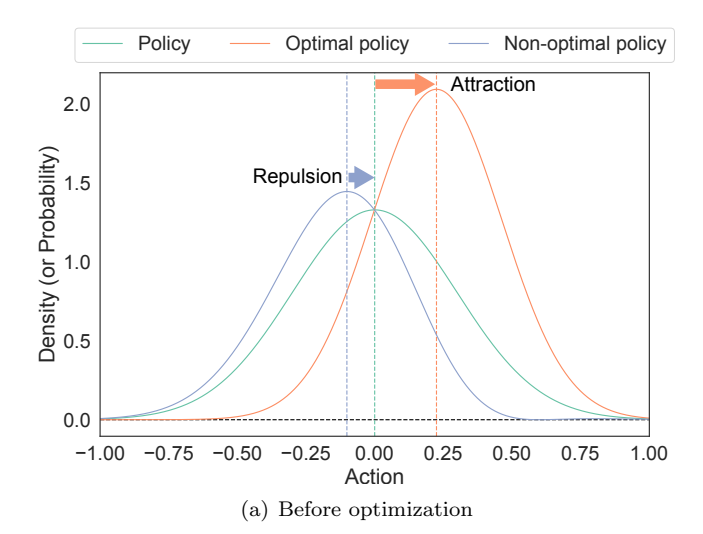
Next, we consider the following minimization problem with forward KL divergence.

$$\min \mathbb{E}_{p_a,b}[\mathrm{KL}(p(O\mid s,a)\mid p(O\mid s))] \tag{14}$$

Similar to the above procedure, the gradient of the forward KL divergence over θ , g_{θ}^{F} , is derived as follows:

$$\begin{split} g_{\theta}^{F} &= -p_{Q}(s, a) \nabla_{\theta} \ln p_{V}(s) - (1 - p_{Q}(s, a)) \nabla_{\theta} \ln(1 - p_{V}(s)) \\ &= -\frac{g_{\theta}^{V}}{\tau} \left\{ p_{Q}(s, a) - \frac{p_{V}(s)(1 - p_{Q}(s, a))}{1 - p_{V}(s)} \right\} \\ &= -\frac{g_{\theta}^{V}}{\tau} \frac{p_{Q}(s, a) - p_{V}(s)}{1 - p_{V}(s)} \\ &\propto -g_{\theta}^{V} \tau \left(\frac{p_{Q}(s, a)}{p_{V}(s)} - 1 \right) \\ &= -g_{\theta}^{V} \tau \left\{ \exp \left(\frac{Q(s, a) - V(s)}{\tau} \right) - 1 \right\} \end{split}$$
(15)

where the proportion is given by multiplying the third line by $\tau^2(1-p_V(s))p_V(s)^{-1}$. Unlike eq. (12), the above equation can directly be computed since C is excluded in the derivation process. The difference with eq. (13) is discussed later in the section 4.



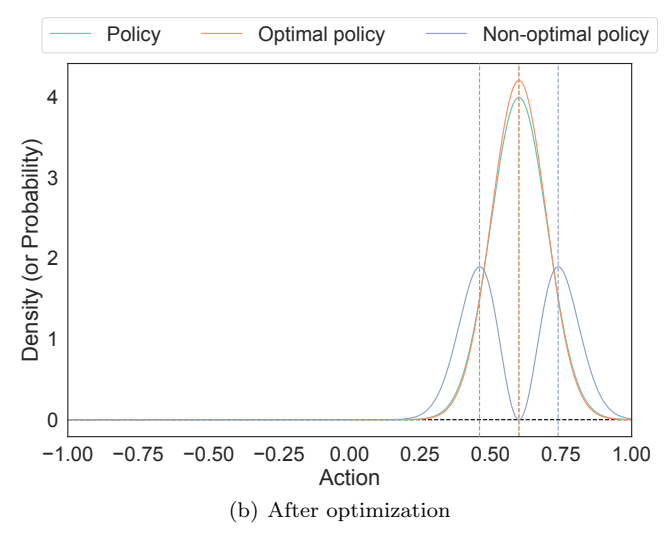


Figure 1: Illustration of optimization problem of policy inspired by triplet loss: (a) the learnable policy is attracted to the optimal policy and repulsed by the non-optimal policy; (b) finally, the learnable policy almost converges to the optimal policy, and the non-optimal policy keeps the learnable policy in place.

3.3. Optimization of KL divergences from optimal/non-optimal policies

From here, the optimization of the policy $\pi(a \mid s)$ with parameter set ϕ is considered. The optimal and non-optimal policies ($\pi^+(a \mid s)$ and $\pi^-(a \mid s)$, respectively) are already given in eq. (10). Using them, an optimization problem is raised such that $\pi(a \mid s)$ approaches $\pi^+(a \mid s)$ and moves away from $\pi^-(a \mid s)$ (see Fig. 1), inspired by triplet loss (Schultz and Joachims, 2003; Chechik et al., 2010). Since we still need to evaluate the divergence between policies as in the case of V(s), the forward/reverse KL divergences are employed again in this paper.

3.3.1. Reverse KL divergence

First, the following minimization problem with reverse KL divergence is solved.

$$\min \mathbb{E}_{p_e}[\mathrm{KL}(\pi(a\mid s)\mid \pi^+(a\mid s)) - \mathrm{KL}(\pi(a\mid s)\mid \pi^-(a\mid s))]$$
(16)

The gradient of the two terms inside the expectation over ϕ , g_{ϕ}^{R} , is derived as follows:

$$g_{\phi}^{R} = \int_{a} \nabla_{\phi} \pi(a \mid s) \ln \frac{\pi(a \mid s)}{\pi^{+}(a \mid s)} - \nabla_{\phi} \pi(a \mid s) \ln \frac{\pi(a \mid s)}{\pi^{-}(a \mid s)} + \pi(a \mid s) \nabla_{\phi} \ln \pi(a \mid s) - \pi(a \mid s) \nabla_{\phi} \ln \pi(a \mid s) da$$

$$= \int_{a} \pi(a \mid s) \frac{\nabla_{\phi} \pi(a \mid s)}{\pi(a \mid s)} \ln \frac{\pi^{-}(a \mid s)}{\pi^{+}(a \mid s)} da$$

$$= \mathbb{E}_{\pi} \left[g_{\phi}^{\pi} \left\{ \frac{V(s) - Q(s, a)}{\tau} + \ln \frac{1 - p_{Q}(s, a)}{1 - p_{V}(s)} \right\} \right]$$

$$\propto \mathbb{E}_{\pi} \left[-g_{\phi}^{\pi} \left\{ (Q(s, a) - V(s)) + \tau \ln \frac{1 - p_{V}(s)}{1 - p_{Q}(s, a)} \right\} \right]$$
(17)

where $g_{\phi}^{\pi} = \nabla_{\phi} \ln \pi(a \mid s)$. The last proportion is given by multiplying the third line by τ .

We can see that the same non-computable term as in eq. (12) appears. In the same way, i.e. by considering the limit of $\tau \to 0$, it can be excluded.

$$g_{\phi}^{R} \simeq \mathbb{E}_{\pi} \left[-g_{\phi}^{\pi}(Q(s, a) - V(s)) \right]$$
$$= \mathbb{E}_{b} \left[-\frac{\pi(a \mid s)}{b(a \mid s)} g_{\phi}^{\pi}(Q(s, a) - V(s)) \right]$$
(18)

where importance sampling (Tokdar and Kass, 2010) is applied to sample a from the baseline policy $b(a \mid s)$. As a result, the minimization problem given in eq. (16) is consistent with the traditional policy gradient method shown in eq. (5), although the sign is inverted due to the difference between maximization and minimization problems.

3.3.2. Forward KL divergence

Next, the forward KL divergence is employed for the following minimization problem.

$$\min \mathbb{E}_{p_e}[\mathrm{KL}(\pi^+(a\mid s)\mid \pi(a\mid s)) - \mathrm{KL}(\pi^-(a\mid s)\mid \pi(a\mid s))]$$
(19)

Similarly, the gradient of the above two terms inside the expectation over ϕ , g_{ϕ}^F , is derived as follows:

$$g_{\phi}^{F} = \int_{a} -\frac{p_{Q}(s,a)}{p_{V}(s)} b(a \mid s) g_{\phi}^{\pi} + \frac{1 - p_{Q}(s,a)}{1 - p_{V}(s)} b(a \mid s) g_{\phi}^{\pi} da$$

$$= \mathbb{E}_{b} \left[-g_{\phi}^{\pi} \left\{ \frac{p_{Q}(s,a)}{p_{V}(s)} - \frac{1 - p_{Q}(s,a)}{1 - p_{V}(s)} \right\} \right]$$

$$= \mathbb{E}_{b} \left[-g_{\phi}^{\pi} \frac{p_{Q}(s,a) - p_{V}(s)}{p_{V}(s)(1 - p_{V}(s))} \right]$$

$$\propto \mathbb{E}_{b} \left[-g_{\phi}^{\pi} \tau \left(\frac{p_{Q}(s,a)}{p_{V}(s)} - 1 \right) \right]$$

$$= \mathbb{E}_{b} \left[-g_{\phi}^{\pi} \tau \left\{ \exp \left(\frac{Q(s,a) - V(s)}{\tau} \right) - 1 \right\} \right]$$
(20)

where the proportion is given by multiplying the fourth line by $\tau(1-p_V(s))$. Without any assumptions, the same term as in eq. (15) is applied to the gradient (for the value function and the log-likelihood of policy, respectively). In addition, the expectation for $b(a \mid s)$ is naturally derived without the importance sampling.

4. Analysis of differences between RKL-RL and FKL-RL

4.1. Qualitative differences between forward/reverse KL divergences

Now, two types of optimization problems using the forward/reverse KL divergences are derived. We refer to the traditional method shown in eqs. (13) and (18) and the new derivation shown in eqs. (15) and (20) as RKL-RL and FKL-RL to easily distinguish between them.

In general, the difference between forward/reverse KL divergences is explained by the way of fitting for its minimization. Specifically, when the learning model has little expressive capability (in particular, the lack of multimodality) for the target distribution, minimization of reverse KL divergence makes the learning model fit into a part of the target. On the other hand, minimization of forward KL divergence tries to fit the learning model on the entire target, resulting in ambiguous model due to the lack of expressive capability.

Due to their properties, given a simple model (e.g. normal distribution), only RKL-RL would acquire one of the local solutions. Inspired by this fact, even imitation learning, which minimizes forward KL divergence, has been converted into the problem for minimizing reverse KL divergence (Ke et al., 2019; Uchibe and Doya, 2020). However, it is not clear whether the obtained local solution has sufficient performance. To find better solutions, the latest RL methods focus on additional regularization problems that make the policy improvement conservative (Schulman et al., 2017) or encourage exploration (Haarnoja et al., 2018).

On the other hand, FKL-RL with the simple model may not acquire any local solutions. Instead, it is expected to explore sufficiently to capture the entire target. The difference in exploration capability affects when the learning model is made more complex like mixture model employed in several practical studies (Kormushev et al., 2010; Daniel et al., 2016; Sasaki and Matsubara, 2019). That is, RKL-RL is prone to local solutions, and even if the number of components is increased, there is no guarantee to make the components fit into different solutions. In contrast, FKL-RL can effectively use all the components to represent the entire target.

Note that the policy optimization in FKL-RL and RKL-RL is not simple minimization problem of forward/reverse KL divergences, it needs to be investigated whether these behaviors can be expected.

4.2. Mathematical differences between RKL-RL and FKL-RL

To clarify the mathematical differences between them, their gradients are summarized as below.

$$\begin{cases}
g_{\theta,\phi}^{R} &= -\mathbb{E}_{p_{e},b}[\delta(s,a)(g_{\theta}^{V} + \rho(s,a)g_{\phi}^{\pi})] \\
\delta(s,a) &:= Q(s,a) - V(s) \simeq r + \gamma V(s') - V(s) \\
\rho(s,a) &:= \pi(a \mid s)/b(a \mid s)
\end{cases}$$

$$\begin{cases}
g_{\theta,\phi}^{F} &= -\mathbb{E}_{p_{e},b}[\tilde{\delta}(s,a)(g_{\theta}^{V} + \tilde{\rho}(s,a)g_{\phi}^{\pi})] \\
\tilde{\delta}(s,a) &:= \tau \left\{ \exp\left(\frac{\delta(s,a)}{\tau}\right) - 1 \right\} \\
\tilde{\rho}(s,a) &:= 1
\end{cases} (22)$$

Note again that $g_{\theta}^V = \nabla_{\theta} V(s)$ and $g_{\phi}^{\pi} = \nabla_{\phi} \ln \pi(a \mid s)$ for simplicity. $\delta(s,a)$ and $\rho(s,a)$ denote TD error and density ratio in the traditional method. $\tilde{\delta}(s,a)$ and $\tilde{\rho}(s,a)$ are regarded as the surrogated versions of $\delta(s,a)$ and $\rho(s,a)$ in FKL-RL, respectively. That is, the differences in RKL-RL and FKL-RL are only in them. The effects of these two differences on learning are discussed in the following sections.

4.2.1. Needs of density ratio regularization on RKL-RL

In RKL-RL (a.k.a. the traditional RL), $\rho(s,a)$ is introduced to change the sampler of action. Although the importance sampling is theoretically acceptable, in terms of numerical stability, the smaller denominator (i.e. likelihood of the baseline policy $b(a \mid s)$) tends to take the larger $\rho(s,a)$, which would diverge the updates of ϕ . It is also known that the approximation performance of expectation with the importance sampling is deteriorated when the alternative sampler (i.e. $b(a \mid s)$) deviates from the original probability (i.e. $\pi(a \mid s)$).

To alleviate these issues in the importance sampling on RKL-RL, the previous studies proposed several methods for regularizing the importance sampling. For example, Munos et al. (2016) clipped $\rho(s,a)$ so as to be within [0,1]. Schulman et al. (2017) (and its modified

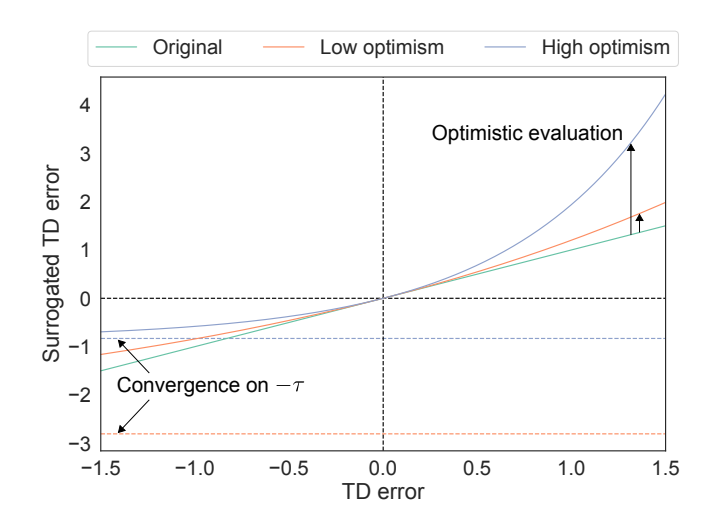


Figure 2: Illustration of (surrogated) TD errors, δ and $\tilde{\delta}$: both δ and $\tilde{\delta}$ always have the same sign; $\tilde{\delta}$ is larger than $-\tau$, two types of which are shown in the dashed lines with the colors corresponding to $\tilde{\delta}$ that have high/low optimism, respectively; as τ becomes smaller, the optimism of $\tilde{\delta}$, i.e. the distance from δ , becomes larger.

version (Kobayashi, 2020b)) regularized the divergence between $b(a \mid s)$ and $\pi(a \mid s)$ by surrogating $\rho(s, a)g_{\phi}^{\pi}$. Compared to FKL-RL, there is room for improvement in the design of $\rho(s, a)$ as above, but its optimization in terms of learning performance is open yet.

4.2.2. Optimistic updates on FKL-RL

 $\delta(s,a)$ and $\tilde{\delta}(s,a)$ are illustrated in Fig. 2. As can be seen in the figure, their signs are reversed at $\delta(s,a) = \tilde{\delta}(s,a) = 0$, and $\tilde{\delta}(s,a)$ is basically larger than $\delta(s,a)$ due to the nonlinearity gained from exponential function.

This nonlinearity leads to optimistic updates on FKL-RL. Mathematically, $\tilde{\delta}(s,a)$ has analytical lower bound: inf $\tilde{\delta}(s,a) = -\tau$. In addition, although $\mathbb{E}_{\pi}[\delta(s,a)] = 0$ since $\mathbb{E}_{\pi}[Q(s,a)] = V(s)$, $\mathbb{E}_{\pi}[\tilde{\delta}(s,a)]$ is non-negative as below.

$$\mathbb{E}_{\pi}[\tilde{\delta}(s, a)] = \tau \mathbb{E}_{\pi} \left[\exp \left(\frac{\delta(s, a)}{\tau} \right) \right] - \tau$$

$$\geq \tau \exp \mathbb{E}_{\pi} \left[\frac{\delta(s, a)}{\tau} \right] - \tau = 0 \qquad (23)$$

where Jensen's inequality is applied to swap exponential and expectation operations. Such positively biased $\tilde{\delta}(s,a)$ would make the value function and the policy optimistically update by acting on their gradients, although $\tilde{\delta}(s,a)=0$ for the ideal policy with Q(s,a)=V(s).

Optimism in RL has long been discussed as a concept to resolve the exploration-exploitation dilemma, and implemented like by optimistic initialization (Machado et al., 2015; Rashid et al., 2020); and increasing the value of exploration using upper confidence (Sunehag and Hutter, 2015; Curi et al., 2020). Recently, optimistic decision making in organisms has been modeled by optimistic RL with asymmetric learning rates and validated (Lefebvre et al.,

2017). In other words, the optimistic updates on FKL-RL have the potential to escape from local solutions and to find global solution efficiently. That is consistent with the behavior of forward KL divergence minimization, which tries to capture the entire target distribution.

4.3. Adaptive design of uncertainty parameter as optimism parameter

One of the main differences in RKL-RL and FKL-RL is the uncertainty parameter, τ , which is left only in FKL-RL. As can be seen in Fig. 2, τ can be interpreted as a coefficient that determines optimism, although the quantitative relationship between them is hard to understand. To intuitively and adaptively design τ , a heuristic conversion of τ is introduced.

The important fact is that $\tilde{\delta}$ has the lower bound inf $\tilde{\delta}(s,a) = -\tau$, and $\tilde{\delta}$ would not change much in the vicinity of this bound, making it difficult to grasp differences in solutions. If we know the scale of δ as Δ , we can design τ by specifying how close $\tilde{\delta}(-\Delta)$ is to the lower bound. Given an alternative parameter $\eta \in (0,1)$, the following design of τ is derived.

$$\tau \left\{ \exp\left(\frac{-\Delta}{\tau}\right) - 1 \right\} = -\eta \tau$$

$$\exp\left(\frac{-\Delta}{\tau}\right) = 1 - \eta$$

$$\tau = -\frac{\Delta}{\ln(1 - \eta)}$$
 (24)

In this design, η is given as a parameter that is more intuitively related to optimism: if $\eta \simeq 0$, the optimistic effect from the exponential function will be vanished, and vice versa. In addition, Δ is expected to be task- and algorithm-dependent, but with this design, there is no need to tune τ for each task with each algorithm.

Instead, Δ for the specific task solved by the specific algorithm is unknown before solving it. In other words, Δ needs to be estimated during training. The estimation is heuristically given as follows:

$$\Delta_{\max} \leftarrow \max(\beta \Delta_{\max}, \max(|\delta|))$$
 (25)

$$\Delta \leftarrow \beta \Delta + (1 - \beta) \Delta_{\text{max}} \tag{26}$$

$$\tau = -\frac{\max(\min(\Delta, \epsilon^{-1}), \epsilon)}{\ln(1 - \eta)}$$
 (27)

where $\Delta_{\rm max}$ stores the recent maximum magnitude of δ , then it is smoothly transferred into Δ . Note that the initial value of $\Delta_{\rm max}$ is given to be ϵ^{-1} as the highest uncertainty, resulting in almost no optimism at the beginning of learning. $\lambda \simeq 1$ is for slowly decaying the past large δ and updating Δ toward $\Delta_{\rm max}$. Since max operator switches the output value discretely, this two-step update provides smooth estimation of Δ and suppresses update fluctuations. In addition, for numerical stability, Δ is clamped using $\epsilon \ll 1$.

5. Integration with methods to accelerate learning

5.1. Prioritized experience replay

The recent standard to accelerate learning is to reuse previous experiences, so-called experience replay (Lin, 1992). Specifically, it stores Markovian data, (s, a, s', r), to a replay buffer with N_c capacity. After finishing each episode, it samples N_b data from the buffer randomly to compute the gradients of parameters and to update them, repeating this process N_e times. As a sampling method, prioritized experience replay (PER) (Schaul et al., 2015), which prioritizes the reuse of important data, has been proposed. PER defines the sampling probability of *i*-th tuple, p_i , based on the magnitude of TD error.

$$w_i = |\delta_i| + \epsilon, \ p_i = \frac{w_i^{\alpha_P}}{\sum_i w_i^{\alpha_P}}$$
 (28)

where ϵ denotes the small value to ensure that $p_i > 0$ and $\alpha_P \geq 0$ is for adjusting the influence of weights. For simplicity, the arguments for TD error, (s,a) are omitted and identified by a subscript i. Note that this weighted sampling can be regarded as importance sampling against uniform distribution, hence in the original paper, the density ratio surrogated by the hyperparameter $\beta_P \in [0,1]$ is multiplied by the loss (or gradient) corresponding to each sample.

In the traditional RL (and RKL-RL), TD error is symmetric, so that both positive and negative values are considered equally important. In FKL-RL, however, we have a new option: instead of δ in eq. (21), $\tilde{\delta}$ in eq. (22) can be used for importance.

$$\tilde{w}_i = |\tilde{\delta}_i| + \epsilon, \ p_i = \frac{\tilde{w}_i^{\alpha_P}}{\sum_i \tilde{w}_i^{\alpha_P}}$$
 (29)

This simple modification indicates that better results are actively reused due to the asymmetry of $\tilde{\delta}$. As a result, a function similar to self-imitation learning (SIL) (Oh et al., 2018), which facilitates exploration by excluding updates with negative TD errors during replay, can be expected.

5.2. Eligibility traces

When FKL-RL is integrated with λ -return and eligibility traces (Sutton and Barto, 2018), we have to consider the fact that the value function in FKL-RL is contained in nonlinear (i.e. exponential) function. To clarify this problem, the definition of generalized advantage estimation (GAE) by Schulman et al. (2016), which is equivalent with λ -return, is first introduced.

$$\delta_t^{\lambda} := \sum_{k=0}^{\infty} (1 - \lambda) \lambda^k \delta_{t+k}$$
 (30)

where $\lambda \in [0, 1]$ denotes the hyperparameter for balancing tradeoff between bias and variance. If this alternates δ in eq. (22), the summation operation is contained in the

exponential function. In that case, GAE itself is naively computable, but eligibility traces, which decompose the summation into terms at each time step and compute them sequentially, cannot be applied theoretically.

To resolve this problem, we can focus on the fact that GAE can be interpreted as the expectation of δ_{t+k} when k is sampled from geometric distribution with parameter $1-\lambda$. That is, Jensen's inequality can be applied as follows:

$$\delta_t^{\lambda} = \tau \frac{\delta_t^{\lambda}}{\tau} = \tau \ln \exp \frac{\delta_t^{\lambda}}{\tau}$$

$$\leq \tau \ln \sum_{k=0}^{\infty} (1 - \lambda) \lambda^k \exp \left(\frac{\delta_{t+k}}{\tau}\right)$$
(31)

Using this inequality, substituting δ_t^{λ} for δ in eq. (22) yields the following relationship.

$$\tau \left\{ \exp\left(\frac{\delta_t^{\lambda}}{\tau}\right) - 1 \right\} \\
\leq \tau \left[\exp\left\{\frac{1}{\tau} \ln \sum_{k=0}^{\infty} (1 - \lambda) \lambda^k \exp\left(\frac{\delta_{t+k}}{\tau}\right) \right\} - 1 \right] \\
= \tau \left\{ \sum_{k=0}^{\infty} (1 - \lambda) \lambda^k \exp\left(\frac{\delta_{t+k}}{\tau}\right) - 1 \right\} \\
= \sum_{k=0}^{\infty} (1 - \lambda) \lambda^k \tau \left\{ \exp\left(\frac{\delta_{t+k}}{\tau}\right) - 1 \right\} \\
= \sum_{k=0}^{\infty} (1 - \lambda) \lambda^k \tilde{\delta}_{t+k} =: \tilde{\delta}_t^{\lambda} \tag{32}$$

As can be seen from the last equation, the surrogated GAE with $\tilde{\delta}_{t+k}$ is derived as the upper bound of $\tilde{\delta}$ with the original GAE. This surrogated GAE can be used for eligibility traces as well as the traditional one since the summation operation is outside of the exponential function. As a remark, when $\tilde{\delta}_t^{\lambda}$ is utilized for updates, optimistic learning occurs here as well.

6. Simulation

6.1. Conditions

The performances of FKL-RL and RKL-RL are investigated through numerical simulations by Pybullet on OpenAI Gym framework (Brockman et al., 2016; Coumans and Bai, 2016). At a first experiment, InvertedDoublePendulumBulletEnv-v0 (abbreviated as DoublePendulum) and HopperBulletEnv-v0 (abbreviated as Hopper) are tried. The higher return may be gained from them as the higher optimism is set since their global solutions exist beyond the off-balance behaviors. In addition, for more realistic robot simulation, MinitaurBulletEnv-v0 (abbreviated as Minitaur) is also tried as a second experiment. Note that its default configurations are modified to be more realistic (see Appendix Appendix A).

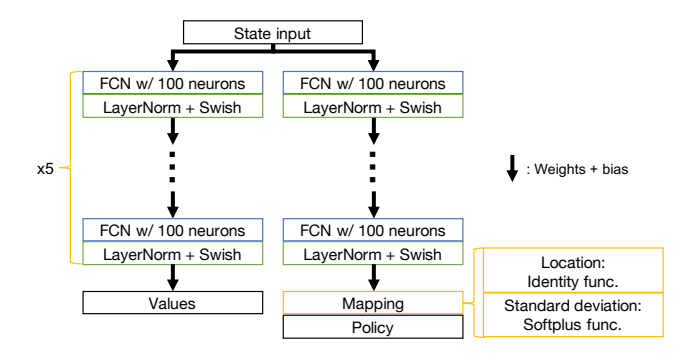


Figure 3: Network architectures for approximating the value function V and the policy π : both functions basically use the same architecture with units of a fully connected layer, layer normalization, and swish activation function; the outputs from the five units are transformed into V and π via a linear transformation by weights and bias and the respective mapping functions.

The network architecture for approximating the value function and the policy is designed using PyTorch (Paszke et al., 2017), as illustrated in Fig. 3. Although the two functions are approximated by separate networks, they share the same basic architecture except for their outputs. Since all the inputs are real values, five fully connected networks (FCNs) are given as hidden layers. Each hidden layer has 100 neurons, and maps to nonlinear space through Layer Normalization and Swish activation function (Ba et al., 2016; Elfwing et al., 2018). Finally, the networks for the value function output five bootstrapped real values, each of which is used for computing δ and averaged. The networks for the policy output a diagonal normal distribution. These networks are optimized by t-Yogi, which integrates Yogi (Zaheer et al., 2018) with t-momentum (Ilboudo et al., 2020), with default configurations except learning rate.

The entropy term of the policy is added to reward as a bonus to stabilize learning, which is equivalent with soft policy gradient (Shi et al., 2019): more specifically, $r \leftarrow r - \tau_H \ln \pi(a \mid s)$ with $\tau_H \geq 0$ gain. Note that -1 in Shi et al. (2019) was omitted since it is a bias term and has no effects analytically. In addition, the target network is introduced for all the networks and updated by t-soft update (Kobayashi and Ilboudo, 2021). The baseline policy $b(a \mid s)$ is therefore set as the output from the target network. Since it has been reported that eligibility traces would not work with nonlinear function approximation, the alternative method that alleviates this problem (Kobayashi, 2020a) is employed. Parameters used in these implementations are listed up in Table 1. Here, the default values are mostly utilized from the previous studies, except the buffer size and the number of drawing from the buffer are reduced due to the limitation of computational resources. Note that the expectation operations introduced above are approximated by Monte Carlo method (i.e. means of data sampled from probabilities listed in subscripts).

Table 1: Common parameters: the two values in curly brackets are those used in the first and second experiments, respectively.

Symbol	Meaning	Value
γ	Discount factor	0.99
α	Learning rate	$\{5 \times 10^{-4}, 5 \times 10^{-6}\}$
ϵ	Minimal value for computational stabilization	10^{-5}
β	Decaying factor for estimation of Δ	0.999
$ au_H$	For entropy maximization (Shi et al., 2019)	0.1
(au_S, u_S)	For t-soft update (Kobayashi and Ilboudo, 2021)	(0.5, 1.0)
$(\lambda_{\max}^1, \lambda_{\max}^2, \kappa)$	For alternative eligibility traces (Kobayashi, 2020a)	(0.5, 0.9, 1.0)
$(N_c, N_e, N_b, \alpha_P, \beta_P)$	For prioritized experience replay (Schaul et al., 2015)	$(10^5, 32, 32, 0.6, 0.4)$

6.2. Results

6.2.1. First experiment

As comparisons in the first experiment, the following five configurations are evaluated.

- RKL-RL (None) as the baseline
- FKL-RL (Zero) with $\tau = \infty$ for no optimism
- FKL-RL (Low) with $\eta = 0.1$ for low optimism
- FKL-RL (Middle) with $\eta = 0.5$ for middle optimism
- FKL-RL (High) with $\eta = 0.9$ for high optimism

By comparing RKL-RL (None) and FKL-RL (Zero), we can see the impact of not having to use importance sampling. By comparing four FKL-RLs, the best balance of the optimism can be found.

Both of DoublePendulum and Hopper were solved by 2000 episodes. In order to evaluate each method with 20 different random seeds, each learned agent is tested 100 times against different initial states. The normalized score (i.e. the sum of rewards), the absolute TD error $|\delta|$, and the log-likelihood of the policy $\ln \pi$ in that test are summarized in Fig. 4. In addition, the convergence of τ in the respective methods and environments is shown in Fig. 5.

First, we can confirm from Fig. 5 that all of cases are sufficiently stationary after roughly 250 episodes, although they converged to different values depending on the specified optimism η and environment (with the specific reward scale). That is, the proposed method can adaptively adjust τ to obtain the specified optimism even when the environment to be solved is changed.

Returning to the learning results in Fig. 4, RKL-RL (None) mostly failed to solve the tasks, and its results were strongly different from the others. By comparing FKL-RL (Zero), we can say that this difference is caused by the existence of importance sampling, which causes numerical instability as mentioned before.

In other results, the learning performance was lower when the optimism is small. This may be due to the lack of optimistic exploration, which leads to a local solution. In contrast, FKL-RL (High) with the maximum optimism obtained smaller $\ln \pi$ than them, suggesting that the stochastic exploration capability was remained until

the end of learning. As a result, FKL-RL (High) achieved the higher scores in all the methods. However, too much optimism deteriorated the learning accuracy of the value function, and according to its inaccurate guide for the policy updates, the variance of scores increased compared to FKL-RL (Middle).

This result may be related to the fact that the poligy gradient method without the baseline term has a large learning variance (Greensmith et al., 2004). That is, as optimism increases, the lower bound of $\tilde{\delta}$, $-\tau$, becomes closer to zero. As a result, most of the information in the direction of worsening the policy, which is not contained in the case without the baseline term (Greensmith et al., 2004), would be lost.

Overall, FKL-RL (Middle) with a moderate optimism achieved the stable performance improvement from RKL-RL and FKL-RL (Zero) without optimism, although the maximum score on Hopper was inferior to FKL-RL (High).

6.2.2. Second experiment

As comparisons in the second experiment, the following two configurations are evaluated.

- FKL-RL with $\eta = 0.5$ for the best optimism
- PPO (Schulman et al., 2017) as the baseline

By this comparison, FKL-RL will be verified to be the one comparable to the state-of-the-art RL method, which is the same implementation used in Kobayashi (2020b) with the same parameters as FKL-RL.

Minitaur was solved by 2000 episodes with 10 different random seeds. Note that, due to the complexity of Minitaur, the learning rate was reduced from 5×10^{-4} to 5×10^{-6} . Learning curves of the sum of rewards as the score, the absolute TD error $|\delta|$, and the log-likelihood of the policy $\ln \pi$ are depicted in Figs. 6(a)–(c), respectively. In addition, almost the best episodes for PPO and FKL-RL are found in an attached video, although their behaviors are not smooth due to observation noise, imperfect PD control, and stochastic behavior.

As can be seen in Fig. 6(a), FKL-RL succeeded in acquiring the forward movement to some extent, while PPO failed. The failure of PPO can be attributed to PER with the smaller buffer size and number of uses ($N_c=10^5$ and

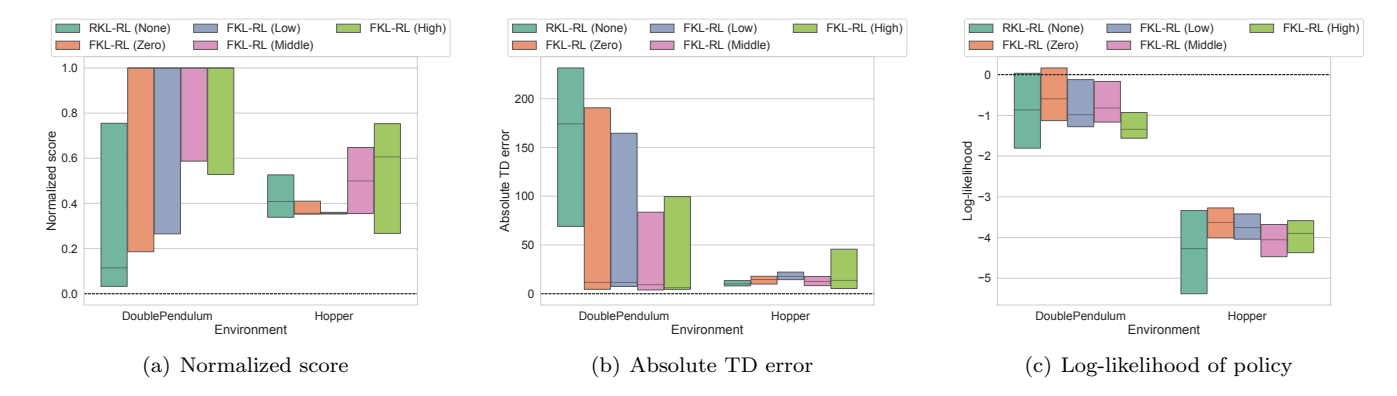


Figure 4: Learning results for the first experiment as boxen plots: all data indicated that RKL-RL failed to learn the given tasks due to numerical instability of importance sampling; (a) normalized sum of rewards can be increased as the optimism η is increased; (b) $|\delta|$ can be reduced correctly even in FKL-RL learned by $\tilde{\delta}$, although too much optimism deteriorated the learning accuracy of the value function; (c) the higher optimism yielded the smaller $\ln \pi$, and therefore, the stochastic exploration capability was remained until the end.

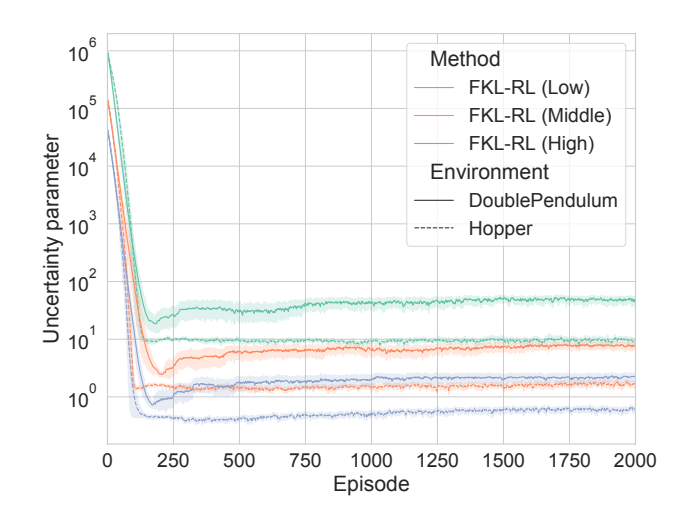


Figure 5: Trajectories of τ in FKL-RL: according to the given optimism η and the solved tasks, the respective methods obtained the different stationary τ ; although the destination of convergence is different, all of them were gained around 250 episodes.

 $N_e=32$) than typical use cases ($N_c\simeq 10^6$ and $N_e>100$). As mentioned above, FKL-RL makes PER more optimistic, which means that the opportunity to learn with less data was effectively utilized in FKL-RL.

Fig. 6(b) shows that FKL-RL has smaller TD error, in other words, it learned the value function more accurately. In addition, the randomness of policy was greater in PPO at the early stage of learning, suggesting that PPO improved the policy more conservatively, while FKL-RL gave relatively high priority to exploitation. These results suggest that FKL-RL was able to estimate the states that would be more valuable earlier than PPO, and prioritize transitions to them, resulting in higher learning efficiency. Note that, in 7 out of 10 random seeds, the probability of the score exceeding 1000 during learning was high, implying that FKL-RL is not prone to getting stuck in local solutions by prioritizing immediate profits.

6.3. Discussion

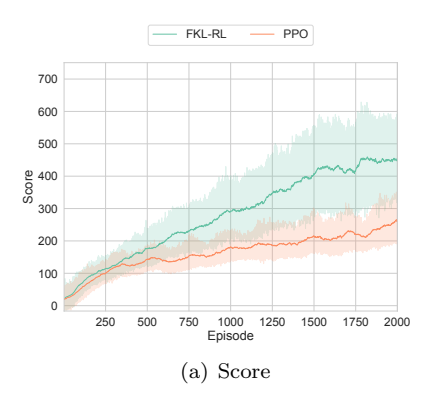
When deriving the optimization problem for policy learning, this paper is inspired by the concept of triplet loss (see again the section 3.3). This gives us a learning rule that is approximately equivalent to the traditional RL when using reverse KL divergence, but open issues with triplet loss are left. One of them is that the policy to be optimized, π , is not necessarily placed between optimal and non-optimal policies, π^+ and π^- . If the gradients away from π^- is stronger than the gradients towards π^+ , π will fail to be optimized. This may be one of the factors that make the policy gradient method unstable. In fact, in the above simulations, the success or failure of learning was affected by random seeds, and this instability has been pointed out in previous studies (Colas et al., 2018; Henderson et al., 2018).

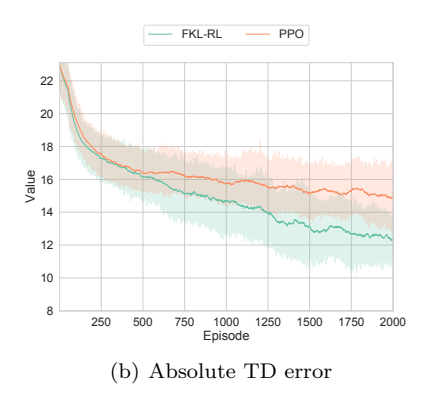
Only if π is sufficiently close to the baseline policy b, this problem can be ignored since b should be placed between π^+ and π^- . Therefore, the recent RL methods (Schulman et al., 2015; Tsurumine et al., 2019; Kobayashi, 2020b) focus on the constraint between π and b, which contributes to the improvement of learning performance. In reality, however, π is not equivalent with b especially during the experience replay.

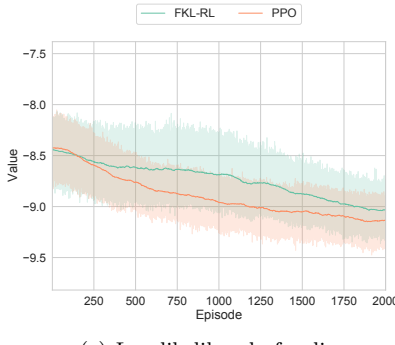
Another direction for solving this issue is to add regularization to the value function so as to force π^+ and π^- to diverge from each other. If this regularization works correctly, it should increase the probability that π is placed between π^+ and π^- , thereby stabilizing policy learning. However, it may make the optimality deterministic too much, and the risk of getting one of the local solutions would be increased.

In the field of metric learning using triplet loss, the solutions to this issue have been proposed. For example, one of them (Cheng et al., 2016) can increase the possibility of making π reach π^+ by adding a minimization problem of the divergence between π and π^+ . The weight of this additional term is however difficult to be designed.

As mentioned above, the fact that policy learning is







(c) Log-likelihood of policy

Figure 6: Learning curves for the second experiment: shaded area denotes 95 % confidence interval; in (a) the sum of rewards, FKL-RL outperformed PPO in this Minitaur task; (b) $|\delta|$ was reduced more efficiently by FKL-RL learned with δ probably due to its moderate optimism; (c) shows that PPO prioritized exploration from the early stage of learning, although that made learning too conservative and caused the failure of increasing the score.

expressed as the triplet-loss-based optimization problem suggests new directions for stabilizing learning. Using the above directions as stepping stones, it is believed that RL can be evolved so as to learn the optimal policy stably without affected by random seeds.

7. Conclusion

This paper addressed a new interpretation of RL as reverse KL divergence optimization, and derived a new optimization method using forward KL divergence, so-called FKL-RL. One remarkable difference was found in FKL-RL that the similar but different learning laws from the traditional RL yield biological optimism. By heuristically converting the original uncertainty parameter τ into the optimism parameter η , the optimism in FKL-RL can be adaptively designed. The effects of this optimism was investigated through learning tendencies on numerical simulations using Pybullet. As a result, the optimism gained by FKL-RL certainly improved the capability to find the global solution by keeping exploration toward probably better situations, although too much optimism caused the increase of learning variance. In more practical robot simulations, FKL-RL was able to obtain performance better than PPO algorithm.

The new derivation of RL, so to speak RL as divergence optimization, makes us expect not only FKL-RL but also methods with different properties derived from other divergences. In the future, this concept will be generalized for arbitrary divergences and investigated towards automatic selection of the task-specific divergence. In addition, a new optimization problem, which solves the problem caused by triplet loss as mentioned in the above discussion, will be derived for more stable learning.

Appendix A. Configurations of Minitaur

MinitaurBulletEnv-v0 abbreviated as Minitaur is for making a quadruped robot walk as fast as possible. Each

Table A.2: Arguments for MinitaurBulletEnv-v0

Name	Default	Modified
motor_velocity_limit	∞	1000
${\tt pd_control_enabled}$	False	True
accurate_motor_model_enabled	True	False
${\tt action_repeat}$	1	4
observation_noise_stdev	0	0.0001
$\mathtt{hard}_{-}\mathtt{reset}$	True	False
${\tt env_randomizer}$	Uniform	None
${ t distance_weight}$	1	200
$\verb"energy_weight"$	0.005	1
${\tt shake_weight}$	0	1
drift_weight	0	1

leg of the quadruped robot has two actuators with velocity limitation (not ∞ in reality), and therefore, the action space is eight-dimensional. In general, the kinematics of the controlled robot is well-known, but the dynamics of the robot (even only actuators) would not be identified precisely. Hence, PD control is employed instead of inverse dynamics. Although the default control period is 100 Hz, due to the limitations of observation, command communication, and/or computation of DRL in real systems, it is reduced to 25 Hz by repeating the same action four times. This task has 28-dimensional state space, and in reality, they are observed with noise. In real robotic systems, hard reset is time-consuming, so it should be omitted. The simulation model is not changed in each episode due to uniqueness of real robot. In summary, the arguments in this task are described in Table A.2. The omitted arguments are with the default values. Note that the weights of the rewards are also adjusted in order to satisfy realistic demands and scale the rewards with other tasks to some extent.

References

- Andrychowicz, M., Wolski, F., Ray, A., Schneider, J., Fong, R., Welinder, P., McGrew, B., Tobin, J., Abbeel, O.P., Zaremba, W., 2017. Hindsight experience replay, in: Advances in Neural Information Processing Systems, pp. 5048–5058.
- Ba, J.L., Kiros, J.R., Hinton, G.E., 2016. Layer normalization. arXiv preprint arXiv:1607.06450.
- Brockman, G., Cheung, V., Pettersson, L., Schneider, J., Schulman, J., Tang, J., Zaremba, W., 2016. Openai gym. arXiv preprint arXiv:1606.01540.
- Chechik, G., Sharma, V., Shalit, U., Bengio, S., 2010. Large scale online learning of image similarity through ranking. Journal of Machine Learning Research 11, 1109–1135.
- Cheng, D., Gong, Y., Zhou, S., Wang, J., Zheng, N., 2016. Person re-identification by multi-channel parts-based cnn with improved triplet loss function, in: Proceedings of the iEEE conference on computer vision and pattern recognition, pp. 1335–1344.
- Chua, K., Calandra, R., McAllister, R., Levine, S., 2018. Deep reinforcement learning in a handful of trials using probabilistic dynamics models, in: Advances in Neural Information Processing Systems, pp. 4754–4765.
- Clavera, I., Fu, Y., Abbeel, P., 2020. Model-augmented actor-critic: Backpropagating through paths, in: International Conference on Learning Representations.
- Colas, C., Sigaud, O., Oudeyer, P.Y., 2018. How many random seeds? statistical power analysis in deep reinforcement learning experiments. arXiv preprint arXiv:1806.08295.
- Coumans, E., Bai, Y., 2016. Pybullet, a python module for physics simulation for games, robotics and machine learning. GitHub repository.
- Curi, S., Berkenkamp, F., Krause, A., 2020. Efficient model-based reinforcement learning through optimistic policy search and planning. Advances in Neural Information Processing Systems 33.
- Daniel, C., Neumann, G., Kroemer, O., Peters, J., et al., 2016. Hierarchical relative entropy policy search. Journal of Machine Learning Research 17, 1–50.
- Elfwing, S., Uchibe, E., Doya, K., 2018. Sigmoid-weighted linear units for neural network function approximation in reinforcement learning. Neural Networks 107, 3–11.
- Fujimoto, S., Hoof, H., Meger, D., 2018. Addressing function approximation error in actor-critic methods, in: International Conference on Machine Learning, PMLR. pp. 1587–1596.
- Greensmith, E., Bartlett, P.L., Baxter, J., 2004. Variance reduction techniques for gradient estimates in reinforcement learning. Journal of Machine Learning Research 5.
- Haarnoja, T., Zhou, A., Abbeel, P., Levine, S., 2018. Soft actorcritic: Off-policy maximum entropy deep reinforcement learning with a stochastic actor. arXiv preprint arXiv:1801.01290.
- Henderson, P., Islam, R., Bachman, P., Pineau, J., Precup, D., Meger, D., 2018. Deep reinforcement learning that matters, in: Proceedings of the AAAI Conference on Artificial Intelligence.
- Ilboudo, W.E.L., Kobayashi, T., Sugimoto, K., 2020. Robust stochastic gradient descent with student-t distribution based first-order momentum. IEEE Transactions on Neural Networks and Learning Systems, 1–14.
- Ke, L., Barnes, M., Sun, W., Lee, G., Choudhury, S., Srinivasa, S., 2019. Imitation learning as f-divergence minimization. arXiv preprint arXiv:1905.12888.
- Kobayashi, T., 2020a. Adaptive and multiple time-scale eligibility traces for online deep reinforcement learning. arXiv preprint arXiv:2008.10040.
- Kobayashi, T., 2020b. Proximal policy optimization with relative pearson divergence. arXiv preprint arXiv:2010.03290 .
- Kobayashi, T., Ilboudo, W.E.L., 2021. t-soft update of target network for deep reinforcement learning. Neural Networks 136, 63–71.
- Kormushev, P., Calinon, S., Caldwell, D.G., 2010. Robot motor skill coordination with em-based reinforcement learning, in: IEEE/RSJ international conference on intelligent robots and systems, IEEE. pp. 3232–3237.
- Kullback, S., 1997. Information theory and statistics. Courier Corporation.

- LeCun, Y., Bengio, Y., Hinton, G., 2015. Deep learning. nature 521, 436.
- Lee, A., Nagabandi, A., Abbeel, P., Levine, S., 2020. Stochastic latent actor-critic: Deep reinforcement learning with a latent variable model. Advances in Neural Information Processing Systems 33.
- Lefebvre, G., Lebreton, M., Meyniel, F., Bourgeois-Gironde, S., Palminteri, S., 2017. Behavioural and neural characterization of optimistic reinforcement learning. Nature Human Behaviour 1, 1–9.
- Levine, S., 2018. Reinforcement learning and control as probabilistic inference: Tutorial and review. arXiv preprint arXiv:1805.00909.
- Levine, S., Pastor, P., Krizhevsky, A., Ibarz, J., Quillen, D., 2018.
 Learning hand-eye coordination for robotic grasping with deep learning and large-scale data collection. The International Journal of Robotics Research 37, 421–436.
- Lin, L.J., 1992. Self-improving reactive agents based on reinforcement learning, planning and teaching. Machine learning 8, 293–321.
- Machado, M.C., Srinivasan, S., Bowling, M.H., 2015. Domainindependent optimistic initialization for reinforcement learning, in: AAAI Workshop: Learning for General Competency in Video Games.
- Modares, H., Ranatunga, I., Lewis, F.L., Popa, D.O., 2015. Optimized assistive human–robot interaction using reinforcement learning. IEEE transactions on cybernetics 46, 655–667.
- Munos, R., Stepleton, T., Harutyunyan, A., Bellemare, M.G., 2016. Safe and efficient off-policy reinforcement learning, in: International Conference on Neural Information Processing Systems, pp. 1054–1062.
- Oh, J., Guo, Y., Singh, S., Lee, H., 2018. Self-imitation learning, in: International Conference on Machine Learning, PMLR. pp. 3878–3887.
- Okada, M., Taniguchi, T., 2020. Variational inference mpc for bayesian model-based reinforcement learning, in: Conference on Robot Learning, PMLR. pp. 258–272.
- Parisi, S., Tangkaratt, V., Peters, J., Khan, M.E., 2019. Td-regularized actor-critic methods. Machine Learning, 1–35.
- Paszke, A., Gross, S., Chintala, S., Chanan, G., Yang, E., DeVito, Z., Lin, Z., Desmaison, A., Antiga, L., Lerer, A., 2017. Automatic differentiation in pytorch, in: Advances in Neural Information Processing Systems Workshop.
- Peng, X.B., Berseth, G., Yin, K., Van De Panne, M., 2017. Deeploco: Dynamic locomotion skills using hierarchical deep reinforcement learning. ACM Transactions on Graphics 36, 1–13.
- Rashid, T., Peng, B., Boehmer, W., Whiteson, S., 2020. Optimistic exploration even with a pessimistic initialisation, in: International Conference on Learning Representations.
- Sasaki, H., Matsubara, T., 2019. Multimodal policy search using overlapping mixtures of sparse gaussian process prior, in: International Conference on Robotics and Automation, IEEE. pp. 2433– 2439.
- Schaul, T., Quan, J., Antonoglou, I., Silver, D., 2015. Prioritized experience replay. arXiv preprint arXiv:1511.05952.
- Schulman, J., Levine, S., Abbeel, P., Jordan, M., Moritz, P., 2015.
 Trust region policy optimization, in: International conference on machine learning, PMLR. pp. 1889–1897.
- Schulman, J., Moritz, P., Levine, S., Jordan, M., Abbeel, P., 2016. High-dimensional continuous control using generalized advantage estimation, in: International Conference on Learning Representations.
- Schulman, J., Wolski, F., Dhariwal, P., Radford, A., Klimov, O., 2017. Proximal policy optimization algorithms. arXiv preprint arXiv:1707.06347.
- Schultz, M., Joachims, T., 2003. Learning a distance metric from relative comparisons. Advances in Neural Information Processing Systems 16, 41–48.
- Shi, W., Song, S., Wu, C., 2019. Soft policy gradient method for maximum entropy deep reinforcement learning, in: International Joint Conference on Artificial Intelligence, pp. 3425–3431.
- Sunehag, P., Hutter, M., 2015. Rationality, optimism and guaran-

- tees in general reinforcement learning. The Journal of Machine Learning Research 16, 1345–1390.
- Sutton, R.S., Barto, A.G., 2018. Reinforcement learning: An introduction. MIT press.
- Tokdar, S.T., Kass, R.E., 2010. Importance sampling: a review. Wiley Interdisciplinary Reviews: Computational Statistics 2, 54–60.
- Tsurumine, Y., Cui, Y., Uchibe, E., Matsubara, T., 2019. Deep reinforcement learning with smooth policy update: Application to robotic cloth manipulation. Robotics and Autonomous Systems 112, 72–83.
- Uchibe, E., Doya, K., 2020. Imitation learning based on entropy-regularized forward and inverse reinforcement learning. arXiv preprint arXiv:2008.07284 .
- Vuong, T.L., Tran, K., 2019. Uncertainty-aware model-based policy optimization. arXiv preprint arXiv:1906.10717 .
- Zaheer, M., Reddi, S.J., Sachan, D., Kale, S., Kumar, S., 2018. Adaptive methods for nonconvex optimization, in: International Conference on Neural Information Processing Systems, pp. 9815–9825.